Diffusion of hydrogen and deuterium on the (110) plane of tungsten

R. DiFoggio* and R. Gomer
The James Franck Institute and the Department of Chemistry, The University of Chicago, Chicago, Illinois 60637
(Received 10 August 1981)

The diffusion of hydrogen and deuterium and of mixtures of these isotopes on the (110) plane of tungsten has been studied by the field-emission-fluctuation method as a function of coverage θ and T. It was possible to show that the results in this system are not influenced by the applied field required for emission. Thermally activated diffusion was found for $T > 130-160$ K, depending on the isotope and θ, with activation energies of $4-5.3$ kcal/mole for ^{1}H (increasing with θ) and marginally but consistently higher values for ^{2}H. Below these temperatures tunneling set in quite abruptly for ^{1}H, and somewhat more gradually for ^{2}H. Values of D_{tun} ranged from 4×10^{-13} to 10^{-12} cm^2/sec depending on θ, for ^{1}H, and from 1.2×10^{-13} to 3.6×10^{-13} cm^2/sec for ^{2}H. The relatively small differences in D_{tun} for ^{1}H and ^{2}H suggest that the tunneling barriers are quite narrow, and these are postulated to correspond to the "necks" between adjacent W atoms. The binding site is postulated to be a long narrow well, corresponding to the "hour-glass"-shaped region between the next nearest W atoms. In the thermally activated regime D increases by over 6 orders of magnitude (at constant T) as θ increases from 0.1 to 0.9 for ^{2}H. A less drastic increase is also found for ^{1}H. The behavior of ^{2}H is tentatively explained by assuming that chemisorbed ^{2}H atoms behave classically, and chemisorbed ^{1}H atoms like fermions, electron spins averaging to 0, so that collisions among adsorbed atoms, leading to very long effective mean free paths are possible at high θ for ^{2}H but not ^{1}H. Evidence for a phase transition, occurring at $80-90$ K depending on θ, was found for both ^{1}H and ^{2}H from an oscillation in the mean-square fluctuation and a corresponding dip in D. It could be shown from supercooling and superheating experiments that the transition is of first order. Evidence of a segregation of ^{1}H and ^{2}H at ~ 130 K in the case of mixtures at high θ is also presented.

INTRODUCTION

The adsorption of hydrogen on metals has been studied in considerable detail, although data on surface diffusion are sparse. In the 1950's Gomer and co-workers obtained some results on the diffusion of H on Ni,[1] and in somewhat more detail on tungsten.[2] However, these results applied to the emitter as a whole rather than to individual crystal planes. The field-emission-fluctuation method developed in this laboratory[3] has made it possible to investigate surface diffusion on single-crystal planes in considerable detail. We report here results for ^{1}H, ^{2}H, and mixtures of these isotopes on the W(110) plane. Although the explanations for some parts of this work remain tentative at best, we consider the results to be sufficiently interesting to warrant publication at this stage. A preliminary account of some very early results has been given.[4,5]

METHOD

The field-emission-fluctuation method for studying surface diffusion has been discussed in some detail previously,[3,6] and we give here only a brief sketch. The method consists of measuring the time autocorrelation function of field-emission-current fluctuations from a small region ($50-100$ Å in radius) of a single-crystal plane, here the (110) plane, which is ~ 1000 Å in diameter. If the emitter is uniformly covered with adsorbate and if the temperature is such that the adsorbate is mobile, statistical adsorbate density fluctuations occur and manifest themselves by fluctuations in the field-emission current. Over the small region examined, the emission-current fluctuations are sufficient to be measured. They build up and decay very approximately with a relaxation time τ_0

defined as

$$\tau_0 = r_0^2/4D \ , \tag{1}$$

where r_0 is the radius of the region probed and D the surface diffusion coefficient of the adsorbate. Consequently, the time correlation function of the density and current fluctuations will decay substantially in time τ_0 and this makes it possible to obtain D. Exact expressions for the density correlation function $f_n(t)$ and for the field-emission —current-correlation function $f_i(t)$ in terms of t/τ_0 have been worked out,[3] and will now be discussed briefly.

The current-correlation function $f_i(t)$ is defined as

$$f_i(t) \equiv \langle \delta \ln i(0) \delta \ln i(t) \rangle \cong \langle \delta i(0) \delta i(t) \rangle / \bar{i}^2 \ , \tag{2}$$

where $\delta i = i - \bar{i}$ and $\bar{i}$ is the average current from the probed region; angular brackets denote ensemble averages. As shown previously,[3] $f_i(t)$ takes the form

$$f_i(t) = \frac{f_n(0)}{A^2} \left[c_1^2 g_1(t) + \left[c_2 \frac{\partial \phi}{\partial c} \right]^2 g_2(t) + 2 \left[c_1 c_2 \frac{\partial \phi}{\partial c} \right] g_3(t) \right] . \tag{3}$$

The quantities c_1, $\partial\phi/\partial c$, and c_2 are related to the parameters occurring in the Fowler-Nordheim equation which governs field emission.[7] We write the latter as

$$\ln i = \ln(B/F^2) - (6.8 \times 10^7/F)\phi^{3/2} \ , \tag{4}$$

where F is the applied field, B is a field-independent quantity, and ϕ is the work function. Then

$$c_1 = \frac{\partial \ln B}{\partial c} \ , \tag{5}$$

$$c_2 = -(\tfrac{3}{2}) 6.8 \times 10^7 (\bar{\phi})^{1/2}/F \ , \tag{6}$$

where c is coverage in atoms/cm^2. The quantities g_1, g_2, and g_3 are correlation functions.[3] g_1, for instance, is proportional to the correlation function for density fluctuations and takes the form

$$g_1(t) = \frac{1}{A} \int_A d^2r \int_A d^2r' \frac{e^{-|\vec{r}' - \vec{r}|^2/4Dt}}{4\pi Dt} \ . \tag{7}$$

A in Eqs. (3) and (7) is the area of the probed region. The quantities g_2 and g_3 are more complicated than g_1 and arise because of contributions of adsorbate dipoles outside the probed region to the potential in A. It is easy to show that g_1, g_2, g_3 can be expressed as functions of t/τ_0. They are defined and their numerical values given in Ref. 3. $f_n(0)$ in Eq. (3) is the mean-square density fluctuation

$$f_n(0) \equiv \langle \delta n(0) \delta n(0) \rangle = Ac^2 K k_B T \ , \tag{8}$$

where K is the two-dimensional compressibility of the ad phase.[8]

It has recently been possible to show[9] that Eq. (3) and the expressions for g_1, g_2, and g_3 initially derived[3] on the assumption of no interactions between adsorbed particles, are also valid when there are interactions and even if more than one phase is present, as long as the wavelengths of fluctuations are much larger than a single lattice spacing, i.e., in the hydrodynamic limit, and that they yield the chemical diffusion coefficient defined by Fick's law.

The procedure for obtaining diffusion coefficients thus consists of obtaining an experimental correlation function $f_i(t)$ and then comparing scaled semilog or more simply log-log plots of the experimental and theoretical functions until coincidence is obtained, thus yielding τ_0 and, to within the accuracy of r_0, D. This procedure also yields $f_n(0)/A^2$ and hence, to within the accuracy of r_0^4, $f_n(0)$. In order to obtain the theoretical curve for $f_i(t)$ according to Eq. (3), the dependence of B and ϕ on coverage must be known. However, the absolute coverage is not required, except for absolute values of $f_n(0)$. Equation (3) can be rewritten as

$$f_i(t) = \frac{f_n(0)}{A^2} \left[\frac{\partial \phi}{\partial c} \right]^2 \left[\left[\frac{\partial \ln B}{\partial \phi} \right]^2 g_1(t) + c_2^2 g_2 + 2c_2 \frac{\partial \ln B}{\partial \phi} g_3(t) \right] \tag{9}$$

by using Eqs. (3) and (5). Thus, all that is required is $\partial \ln B / \partial \phi$ over the coverage range of interest. It turns out that $\partial \ln B/\partial\phi$ is constant in the present case.

EXPERIMENTAL

The experimental tube, shown in Fig. 1, is a modification of apparatus used previously,[6] and provides for optical decoupling between the signal to be detected and the field-emission tube. The beam from the emitter is steered in the usual manner[6] by electrostatic deflection plates until the

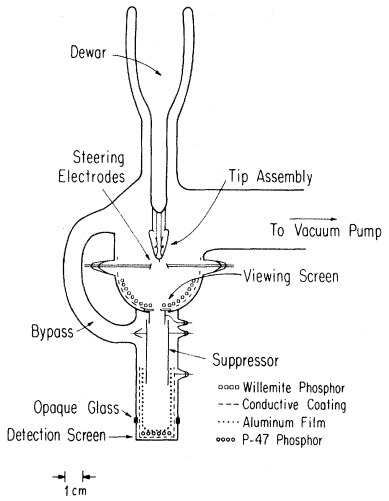

FIG. 1. Schematic diagram of field emission tube for fluctuation measurements. Only one set of electrostatic deflection (steering) electrodes is shown.

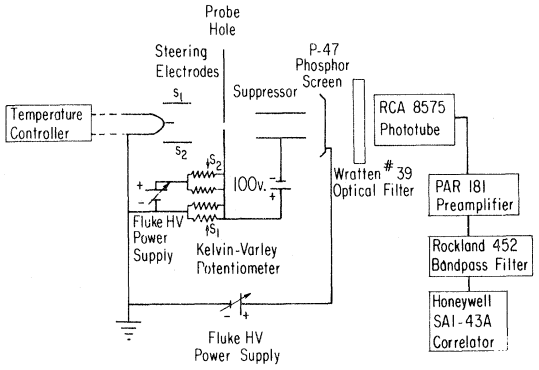

FIG. 2. Schematic block diagram of correlation measurements.

desired region is located over the probe hole. The currect from the probed region then passes through a suppressor to prevent secondary electrons from the edge of the probe hole from reaching the fast phosphor. After passage through the suppressor the beam is accelerated to a voltage of 8—10 kV and allowed to impinge on a P-47 phosphor screen, which has a 100 nsec decay time. Thus its light output follows the current fluctuations whose decay times, by suitable choice of emitter temperature, are less than 10^{-3} sec. The phosphor is backed with a ~1500-Å-thick layer of Al to prevent stray light from reaching the phototube externally mounted beneath it. A section of opaque glass (Fig. 1) also prevents light piped within the glass envelope from reaching the phototube. The phosphor used for the main screen was willemite, emitting in the green, while the P-47 phosphor produces violet-blue light. Stray light was further reduced by placing a sharp band pass filter (Wratten No. 39) in front of the RCA8575 phototube. The latter was magnetically shielded and also electrostatically shielded from the field-emission tube by means of a thin plate of electrically conducting transparent glass, kept at the potential of the phototube's photocathode. The electrical arrangement used is shown in Fig. 2.

The current gain of the P-47 phosphor-phototube combination was estimated as 5×10^3 under most operating conditions. The gain could have been increased by at least a factor of 10 by increasing both electron accelerating and phototube voltages, but the values used maximized signal-to-noise ratio for correlation measurements. The sensitivity of the PAR181 preamplifier was 10^7 V/A and a final voltage gain of 100 was used in the filter stage. The low-frequency cutoff of the latter was always set at 0.01 Hz. The high-frequency cutoff was set at the sampling frequency of the Honeywell SAI-43A correlator for a given run. This helped to improve signal-to-noise ratio considerably and thus reduced acquisition times for correlation functions. The independence of correlation functions of the values of high-frequency cutoffs above the sampling frequency was verified experimentally. The correlator takes 400 current measurements at preset intervals (i.e., at preset sampling frequency), so adjusted as to span the decay of f_i to at least 50% of its initial value. This depends, of course, on the value of τ_0, i.e., D, which is a function of temperature. The number of summations for each datum point was 10^5 to 3×10^6, depending on signal size. Acquisition times of correlation functions varied from 10—60 min.

The frequency response of the system was tested by applying a small ac signal of variable frequency to the emitter and measuring the ac output of the PAR preamplifier. It was found to be constant to 20 kHz, a frequency considerably higher than required. The dc probe-hole current was measured by passing the output of the phototube directly into a Dymec 2211B voltage-to-frequency converter, using the accurate 1 MΩ±0.01% input resistor of this unit as a load resistor. The output of the converter was then read on a scaler. Total emitter current was measured similarly.

Temperature control was accomplished by filling the Dewar shown schematically in Fig. 1 with liquid N_2 or liquid H_2 and heating the emitter loop resistively, with a temperature controller described previously.[6] The tube was attached to a Varian

stainless steel vacuum system, pumped by iron and Ti sublimation pumps. The Viton O-ring of the poppet valve in this system was removed to improve ultimate vacuum. Gases were admitted via Varian variable leak valves directly attached to the system. A UTI C-100 quadrupole mass spectrometer in the system made it possible to monitor residual gases and ^1H and ^2H purity. Spectroscopic grade gases in Pyrex bottles were used without further purification and proved to be free from detectable impurities, except for $\sim 1\%$ of ^1H in the deuterium. After bakeout at 250°C the base pressure in the system was 2×10^{-11} torr as indicated by the ion gauge and also by contamination rates of the emitter.

Two dosing procedures for ^1H or ^2H alone were followed and gave identical results. In each procedure the emitter was first cleaned by flashing in the conventional way. In procedure 1 the emitter was then cooled to 80 K and the hydrogen or deuterium pressure raised to 5×10^{-9} torr (as read without corrections on the ion gauge) for 50–200 sec. It is known from the work of Polizotti and Ehrlich[10] that H_2 is only weakly adsorbed on (110) and desorbs without dissociation at $T<40$ K. Thus the stably adsorbed species, atomic H, reaches the (110) plane (in the absence of imperfections, which permit dissociative adsorption on macroscopic planes) only by diffusion from the atomically rough vicinals where H_2 does adsorb dissociatively. Since diffusion of H into the plane at 80 K is very slow, the emitter was heated to 200–250 K until the desired coverage on (110) was reached, as indicated by the emission current (always checked, however, by an actual work-function determination). In procedure 2, dosing was carried out at 200–300 K and the entire emitter equilibrated with respect to H coverage. It was found that for diffusion measurements appreciably below the influx temperature no changes in coverage on (110) occurred in the times of the diffusion measurements, so that both methods gave the same results for equal coverages on (110). The constancy of coverage was checked, as already indicated, by work-function measurements before and after diffusion runs.

RESULTS AND DISCUSSION

Effect of applied field on diffusion

The dosing procedure just described also made it possible to check the effect of applied field on diffusion by monitoring the current at the center of the (110) plane as a function of time when H was allowed to diffuse into the plane at 180 K (a) with the field applied continuously and (b) with the field turned on only at intervals, the temperature being reduced 80 K before the field was turned on. Identical plots of current change versus time resulted, indicating that the applied field has no appreciable effect on diffusion in this system.

Work function and Fowler-Nordheim parameters

Figure 3 shows $\Delta \ln B$ vs $\Delta\phi$ (as H coverage is varied from 0 to maximum), obtained from plots of $\ln i/V^2$ vs $1/V$ for the probed region and Eq. (4), assuming a value of $\phi(110)=5.3$ eV for the clean plane. The maximum work-function change for H adsorption, -0.5 eV, is in good agreement with previous work.[10,11] No differences in emission current or $\Delta\phi$ were found between ^1H and ^2H, at maximum coverage. For the (110) plane maximum coverage was also found to be independent of whether the emitter had been dosed and equilibrated at 200 or 300 K, although decreases in $\Delta\phi$ for some other planes were noted when a saturated emitter was heated from 200 to 300 K. If it is assumed that maximum coverage on (110) corresponds to H/W=1 or to an absolute coverage of 1.42×10^{15} H atoms/cm^2, the data of Fig. 2 yield the following values for the constants entering into Eq. (3): $c_1=-1.58\times 10^{-15}$ cm^2; $\partial\phi/\partial c = -3.52\times 10^{-16}$ eV cm^2. The assumption that $\theta=1$ corresponds to H/W=1 is supported by the low-energy electron diffraction (LEED) observations of Naumovets and co-workers,[12] and also by those of Menzel and co-workers[13] who find a

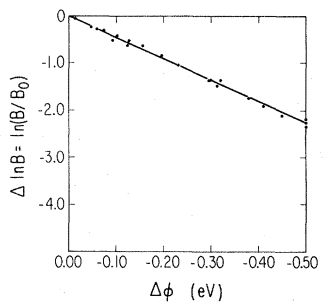

FIG. 3. Plot of $\Delta \ln B$ vs $\Delta\phi$ on the W(110) plane as H coverage is increased. B is defined in Eq. (4) and B_0 refers to its value for the clean surface.

$p(1\times1)$ pattern at maximum coverage with various other structures at intermediate θ.

The value of r_0 was determined by the method described in detail in Ref. 6 from the relation between the average field-voltage proportionality constant $\bar{k}=F/V$ and the tip radius r_t:

$$r_t=0.29/\bar{k} \tag{10}$$

for the electrode geometry used in the present microscope tube. The radius of the probed region r_0 is then found from

$$r_0=r_p r_t\beta/x\ , \tag{11}$$

where r_p is the radius of the probe hole (0.75 mm), x is the tip-to-probe-hole distance ($\sim$3.9 cm), and β is a compression factor ($\sim$1.5) determined from the apparent angular separation of some of the principal crystallographic directions in the emission pattern. $\bar{k}$ is determined from

$$\bar{k}=-6.8\times10^7\phi_c^{3/2}/S_c \tag{12}$$

where $\phi_c=4.5$ eV is the average work function of clean W and S_c is the slope of $\ln i/V^2$ vs $1/V$ plots for the whole emitter. $r_0\sim100$ Å in the present measurements.

The field on the (110) plane required for evaluation of c_2 was found from the applied voltage V and k_{110} which is obtained from the relation

$$k_{110}/\bar{k}=(5.3/\phi_{\rm app})^{3/2} \tag{13}$$

where $\phi_{\rm app}$ is the apparent work function obtained from a Fowler-Nordheim plot for the (110) plane using the average field-voltage proportionality constant $\bar{k}$. $\phi_{\rm app}\cong5.8$ eV, yielding a reduction in field on the (110) plane of $\sim$17%. The value of c_2 obtained in this way was $c_2=-5.45$ (eV)$^{-1}$.

Diffusion results

Figure 4 shows a typical correlation function and Figs. 5 and 6 superpositions of log-log plots of experimental and theoretical curves. The fit is seen to be excellent. In some cases vertically scaled semilog plots of f_i were compared with the theoretical curves, since this permits a slightly easier determination of τ_0; no appreciable difference in the accuracy of the two methods was found (Fig. 7).

Figure 8 shows a summary of diffusion data for ^{1}H and ^{2}H for relative coverages $\theta=0.1$, 0.3, 0.6, and 0.9. These θ values are based on the assumption that $\Delta\phi$ varies linearly with c so that

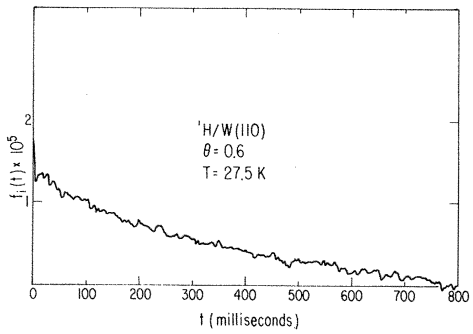

FIG. 4. A typical correlation function, $f_i(t)$ vs t. Experimental conditions are indicated on the figure.

$$\theta=\Delta\phi/\Delta\phi_{\rm max}\ . \tag{14}$$

The fact that $\Delta\ln B$ vs $\Delta\phi$ is linear (Fig. 3) supports this assumption, but does not guarantee it, of course. For ^{2}H at $\theta=0.1$ the signal was quite weak and for $T<130$ K the fluctuations were so slow as to be unmeasurable with the apparatus at our disposal. Further, over the very long times required to obtain a meaningful correlation function, small amounts of ^{1}H contamination, even at the low base pressure in the system, led to spurious results. The $\theta=0.1$ curve for ^{2}H is therefore incomplete.

The data of Fig. 8 show several striking features. For $138<T<160$ K, depending on θ, diffusion is activated, i.e., temperature dependent for both isotopes. Below these temperatures D is virtually temperature independent to the lowest measured value $\sim$30 K, except for a dip near 80–90 K. The location of this dip is a function of coverage. It will be shown to be associated with a phase transition and will be discussed in detail later.

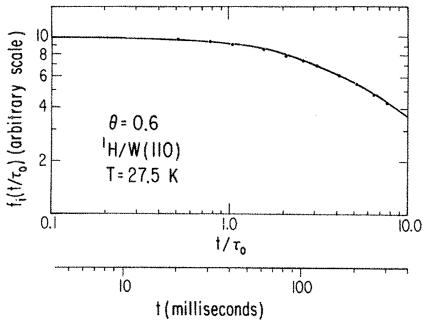

FIG. 5. Comparison of experimental and theoretical current correlation functions by means of superimposed log-log plots. Experimental conditions are indicated on the figure. Solid line: theoretical curve. Points: experimental data.

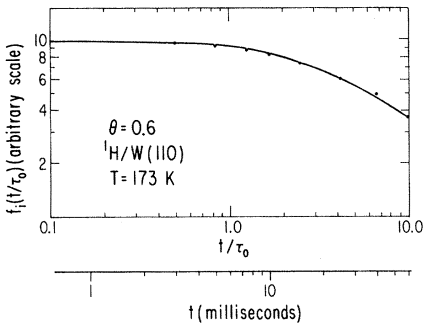

FIG. 6. Comparison of experimental and theoretical current correlation functions by means of superimposed log-log plots. Experimental conditions are indicated on the figure. Solid line: theoretical curve. Points: experimental data.

In the thermally activated regime D varies with coverage θ, the variation being much stronger for ^{2}H than for ^{1}H. If D in this regime is decomposed into a temperature-dependent and a temperature-independent part,

$$D = D_0 e^{-E/k_B T}, \tag{15}$$

the results shown in Table I and in Figs. 9 and 10 are obtained. E varies only very slightly with θ for both ^{1}H and ^{2}H, while D_0 varies strongly. For ^{1}H, $\log_{10} D_0$ vs θ consists of two linear regimes, the variation being relatively slight for $0.3 < \theta < 0.9$ and quite steep for $\theta < 0.3$; for ^{2}H, $\log_{10} D_0$ vs θ is linear over the entire θ regime investigated. It is also remarkable that for ^{2}H D_0 spans almost 6 orders of magnitude with increasing θ, while only 3 orders are spanned for ^{1}H. At each coverage E is slightly but significantly higher for ^{2}H than for H.

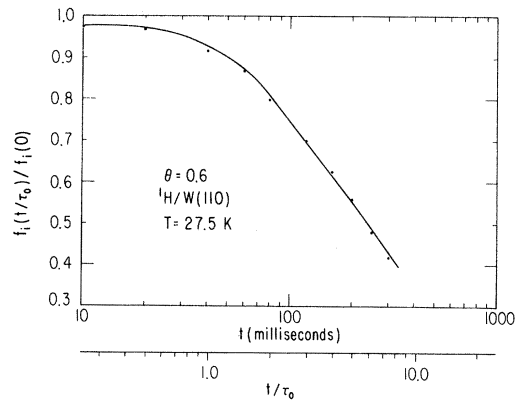

FIG. 7. Comparison of experimental and theoretical current correlation functions by means of semilog plots with ordinates scaled for best fit. Solid line is the theoretical curve; points are experimental values.

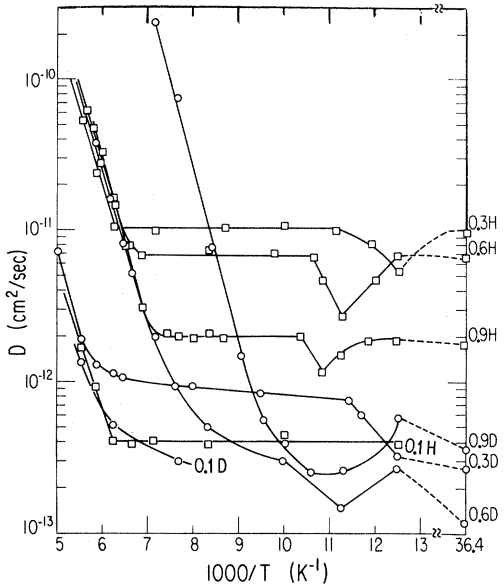

FIG. 8. Plots of $\log_{10} D$ vs $1/T$ for hydrogen and deuterium at various fractional coverages, indicated by the numbers to the right of each curve. Dashed lines represent interpolations between 80 and 27 K, where no data were taken. ^{1}H is marked H, ^{2}H is marked D on the curves.

In the temperature-independent regime D is also a function of θ for both ^{1}H and ^{2}H (Fig. 11), although the functional dependence differs for the two isotopes. For ^{1}H, D seems to have a maximum at $\theta = 0.3$ and then decreases monotonically. For ^{2}H there seems to be a minimum at $\theta = 0.6$; D also seems to vary less in absolute magnitude with θ for ^{2}H. The decrease in D with θ for $\theta < 0.3$ for both ^{1}H and ^{2}H seems quite surprising and was therefore checked with different emitters but found to be real. For ^{2}H the dip at 80–90 K already noted also occurs, although it seems to be rather broader at $\theta = 0.9$ than for ^{1}H. For ^{2}H, D is slightly temperature dependent even at low T. Finally, the (nearly) temperature-independent regime gives much higher values of D for ^{1}H than for ^{2}H, particularly if the same coverages are compared.

The qualitative explanation of all the features just presented, except the coverage dependence of D_0 for thermally activated diffusion, seems reasonably clear. At "high" temperatures activated diffusion occurs for both ^{1}H and ^{2}H, with an activation energy of ~ 5 kcal/mole, i.e., ~ 0.2 eV. [Incidentally, this value agrees very closely with that obtained in 1957 by Wortman, Gomer, and Lundy[2] for the diffusion on the vicinals of (110), 5–6 kcal, and even the value of $D_0 = 1.8 \times 10^{-5}$

TABLE I. Activation energies (kcal/mol) and prefactors (cm^2/sec) in the thermal regime for H/W(110).

	Single isotopes	
	100 at.% ^{1}H	100 at.% ^{2}H
$\theta=0.1$	$E_A=4.07\pm0.13$ $D_0^{\text{therm}}=1.55\times10^{-7}$	$E_A=(4)$ (est.) $D_0^{\text{therm}}=(10^{-7})$ (est.)
$\theta=0.3$	$E_A=4.67\pm0.15$ $D_0^{\text{therm}}=2.50\times10^{-5}$	$E_A=4.76\pm0.30$ $D_0^{\text{therm}}=1.16\times10^{-6}$
$\theta=0.6$	$E_A=4.80\pm0.30$ $D_0^{\text{therm}}=5.0\times10^{-5}$	$E_A=4.85\pm0.15$ $D_0^{\text{therm}}=5.8\times10^{-5}$
$\theta=0.9$	$E_A=5.10\pm0.10$ $D_0^{\text{therm}}=1.48\times10^{-4}$	$E_A=5.35\pm0.12$ $D_0^{\text{therm}}=5.85\times10^{-2}$

	Mixtures		
	75 at.% ^{1}H−25 at.% ^{2}H	50 at.% ^{1}H−50 at.% ^{2}H	25 at.% ^{1}H−75 at.% ^{2}H
$\theta=0.9$	$E_A=4.03\pm0.11$ $D_0^{\text{therm}}=3.42\times10^{-6}$	$E_A=4.04\pm0.10$ $D_0^{\text{therm}}=2.73\times10^{-6}$	$E_A=7.4$ $D_0^{\text{therm}}=0.35$

$cm^2\,sec^{-1}$ reported by these authors is in the range of values found here at different coverages.] As temperature decreases, tunneling of H *through* the potential barrier becomes competitive with activated diffusion and soon dominates. Tunneling must have an exponential dependence on $m^{1/2}$, m being the mass of the tunneling particle, and thus must be considerably less probable for ^{2}H than for ^{1}H. Consequently the switch to tunneling should occur at lower temperatures and should also result in lower values of D for ^{2}H than for ^{1}H, as is in fact observed.

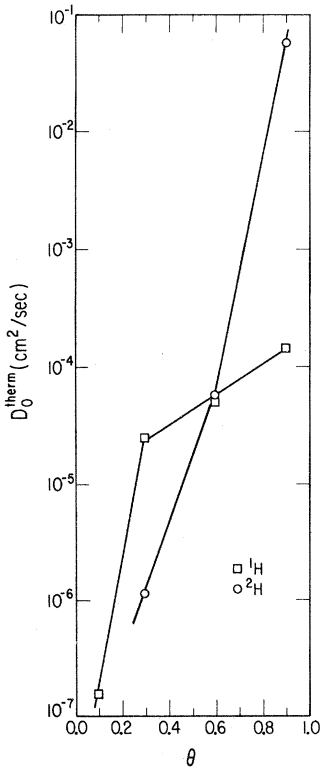

FIG. 9. $\log_{10}D_0$ vs relative coverage θ for hydrogen and deuterium in the thermally activated regime.

Tunneling regime

We shall discuss first the tunneling results. In a preliminary publication,[4] it was assumed that the appropriate formalism is that of tunneling from a

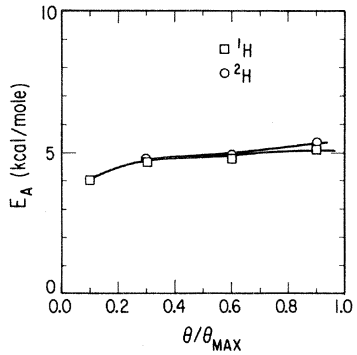

FIG. 10 Activation energy of diffusion in the thermally activated regime vs relative coverage for hydrogen and deuterium.

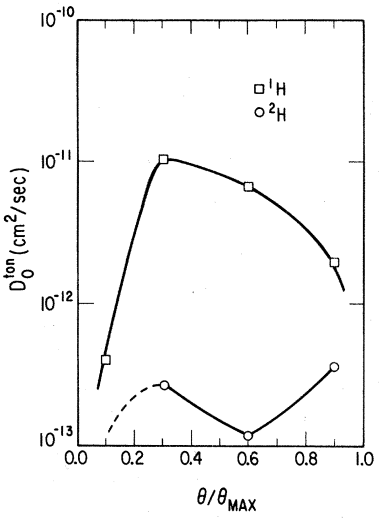

FIG. 11. Diffusion coefficients in the tunneling regime vs relative coverage for hydrogen and deuterium. For ^{2}H the values of D at 27 K were used.

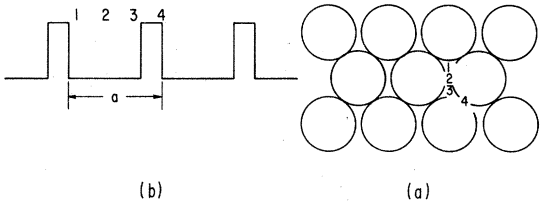

FIG. 12. (a) Top view of (110) plane; various positions indicated by numbers. (b) Schematic one-dimensional potential-energy diagram for translation of chemisorbed hydrogen parallel to this plane. Numbers correspond to those in (a).

discrete state to a continuum as, for instance, in field emission. However, at least at low coverage, it seems more appropriate to assume tunneling from a given state in a well into an equivalent state in an adjacent well, so that a band picture is appropriate. Then the group velocity v_g is

$$v_g = \frac{1}{\hbar}\frac{\partial E}{\partial k} \tag{16}$$

and the diffusion coefficient can be written as

$$D = v_g \lambda , \tag{17}$$

where λ, the mean free path, is adequately approximated by

$$\lambda \cong c^{-1/2} , \tag{18}$$

c being coverage in atoms/cm^2 as before. Since W has a Debye temperature very much higher than that at which tunneling is observed, the assumption that λ is limited by adsorbate-adsorbate rather than by adsorbate-phonon collisions seems justified.

At this point some discussion of the assumed binding sites and position of the barrier is in order. Figure 12(a) shows the geometry of the (110) plane. It is generally believed that the bridge position between two nontouching atoms, corresponding to position 2 on Fig. 12(a), is the stable binding site for H on the (100) plane, where this corresponds to the position between edge atoms of the unit square. It therefore seem reasonable to assume that this is also the site of lowest energy on (110). Some work by Backx, Feuerbacher, Fitton, and Willis[14] seems to show that two vibrational loss peaks at 95 and 157 meV, respectively, occur on (110) at all coverages. Backx *et al.* interpreted this result as indicating the occupation of two distinct binding sites at all coverages. This hypothesis, however, is irreconcilable with the fact that a $p(1\times1)$ LEED pattern results[12,13] at $\theta=1$ and is also implausible on thermodynamic grounds. There is no reason to suppose that both sites would have equal free energy, so that at low θ and low T only the more tightly binding site should be appreciably occupied. It seems far more likely that these authors, in fact, observed the normal stretching mode at 157 meV and a bending mode, probably that corresponding to V_2 or V_3 on (100) (using the notation of Ho, Willis, and Plummer[15]). On the (110) plane one of these modes could easily have a change in dipole moment normal to the surface.

It is also clear that the barrier, if its height is given by $\sim$0.2 eV, i.e., the thermal activation energy, must be quite narrow. If this were not so, the ratio of hydrogen to deuterium diffusion coefficients in the tunneling regime would have to be much larger than that observed. Consequently we will take as a first approximation to the potential the rectangular well and barrier depicted in Fig. 12(b), identifying the well with the hourglass region 1-2-3 in Fig. 12(a) and the barrier with the necks between adjacent W atoms [marked 4 in Fig. 12(a)]. The potential surface thus consists of two nonorthogonal quasi-one-dimensional periodic structures and hence of a two-dimensional band, but we ignore the nonorthogonality for the present. Since a nearest-neighbor tight-binding approximation surely suffices here, we can write

$$v_g = (a/\hbar)\langle V\rangle \sin ka \tag{19}$$

where a is the lattice periodicity, k is the one-dimensional wave vector, and $\langle V\rangle$ is the tight-binding matrix element. If we assume for simplici-

ty $\sin ka \sim 1$, i.e., assume that the tunneling band is so narrow that the occupation of all allowed levels within the band is equally probable, we find for D

$$D=(a/\hbar)\langle V\rangle c^{-1/2} . \tag{20}$$

The matrix element $\langle V\rangle$ consists of the integral over the region indicated schematically in Fig. 13. For the ground-state function $\cos k_0 x$ in each well $\langle V\rangle$ is given by

$$\begin{aligned}\langle 0\,|\,V\,|\,0\rangle &= -VB^2 e^{-k(l_0+b)}\int_{-b}^{b} e^{-kx}\cos k_0 x\,dx \\ &\cong VB^2 e^{-kl_0}\frac{k\cos k_0 b + k_0 \sin k_0 b}{k^2+k_0^2} \\ &\equiv \alpha e^{-kl_0} ,\end{aligned} \tag{21}$$

since the upper limit of the integral can be neglected relative to the lower limit. Here B is the amplitude of the wave function at the classical turning point, V is the depth of the well, and

$$k=(2m/\hbar^2)^{1/2}V^{1/2} . \tag{22}$$

Thus the dominant contribution to V and hence to the diffusion coefficient is the exponential term

$$\exp\{-[(2m/\hbar^2)^{1/2}V^{1/2}l_0]\} . \tag{23}$$

Expression (23) is valid for a rectangular barrier; in general it would be given by

$$\exp\left[-\left[[2m(\hbar^2)^{1/2}]\int_{x_1}^{x_2}\sqrt{V(x)-E}\,dx\right]\right] \tag{24}$$

at least in terms of the WKB approximation, x_1 and x_2 being the appropriate classical turning points. Expressions (23) and (24) are just the square roots of the leading term in the "ordinary" tunneling expression. This is to be expected since the latter can be shown, for instance, by the transfer Hamiltonian formalism to be formally equivalent to Fermi's golden rule, and thus to contain $|\langle V\rangle|^2$.

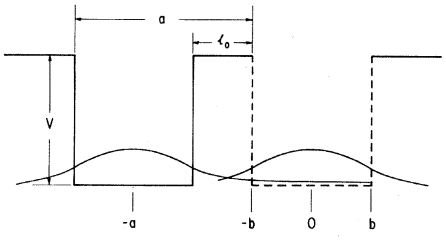

FIG. 13. Schematic diagram indicating the calculation of the matrix element $\langle V\rangle$ described by Eq. (21) in the tight-binding approximation with neglect of all but nearest-neighbor contributions. The perturbing potential in this approximation is indicated by the dashed lines and the integral in Eq. (21) runs from $-b$ to $+b$. Also indicated schematically are the relevant wave functions. The repeating length is a, the well depth is V, the well width is $2b$, and the barrier width is l_0.

The discussion to this point has ignored H-H interactions, except to assume that these limit the mean free path. The quite different dependence of D on θ for ^{1}H and ^{2}H in the tunneling regime indicates that this is a gross oversimplification and that more subtle effects than a variation of the barrier dimensions by H-H interactions must play a role. Formally, these interactions can be treated by assigning effective masses which would then directly appear in Eq. (22). The origin of the interactions giving rise to this renormalization and in particular to the difference between ^{1}H and ^{2}H is not understood. It is probably connected in part with the different statistics of the isotopes. A statistical argument will be invoked later to explain the differences in the thermal behavior. All these effects, however, should become unimportant at sufficiently low coverage.

Well and barrier dimensions

If the potential structure could be adequately approximated by Fig. 12, it would now be simple to find the appropriate values of k_0 for ^{1}H and ^{2}H and to obtain the barrier width l_0 from the ratio of D for the two isotopes:

$$\frac{D(^1\mathrm{H})}{D(^2\mathrm{H})}=\frac{\alpha(^1\mathrm{H})}{\alpha(^2\mathrm{H})}\exp[(\sqrt{2}-1)(2m_1/\hbar^2)^{1/2}V^{1/2}l_0] . \tag{25}$$

Here the experimental tunneling diffusion coefficients would be used; V can be taken as the activation energy obtained from the thermal regime and m_1 is the mass of ^{1}H. The ratio $\alpha(^1\mathrm{H})/\alpha(^2\mathrm{H})$ [α is defined in Eq. (21)] depends only slightly on b and is $\sim\frac{1}{2}$. For this purpose it is of course desirable to compare D values at the lowest coverage available to avoid effects of ad-ad interactions which differ for ^{1}H and ^{2}H, as already noted. However, even this is not enough. The slight but unmistakable temperature dependence of D for ^{2}H necessitates a more complicated model. The fact that there is a temperature dependence for ^{2}H but not for ^{1}H suggests that the idealized well may not be flat-bottomed but contains a dip in the middle as shown in Fig. 14. Because of its lighter mass, ^{1}H could then have no bound state in the subsidi-

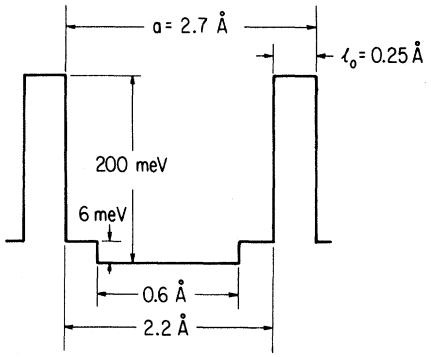

FIG. 14. One-dimensional double well structure with best fits for $\theta=0.3$, indicated on the figure.

ary well, while ^{2}H could. Thus ^{2}H tunneling could be temperature dependent, for instance, if tunneling from the bound state in the subsidiary well was much less likely than from the next state lying above the subsidiary well. The actual geometry of the (110) plane, shown in Fig. 12, makes the possibility of a subsidiary well plausible.

For the case of a subsidiary well, shown in Fig. 14, a fit to the experimental curve for ^{2}H at $\theta=0.3$ could be obtained only by assuming that tunneling from the ground state [0] was $<10\%$ of tunneling from state [1], which is not bound in the subsidiary well. For this case the temperature-dependent diffusion coefficient in the tunneling regime, $D(T)$, is given by

$$D(T)=D_1(e^{\epsilon/k_BT}+1)^{-1}, \tag{26}$$

where ϵ is the energy difference between the states [0] and [1]. A very good fit was obtained for $\theta=0.3$ with $\epsilon=189$ cal/mole, i.e., ~ 8 meV.

Unfortunately, as already pointed out, it is not possible to make the comparable calculation at $\theta=0.1$ since the curve for ^{2}H is incomplete. It seems quite clear, however, that the value of 8 meV is a factor of 10 smaller than the vibrational energy of 95 meV observed by Backx *et al.*[14] If our model is even approximately correct, this would indicate that the vibration at 95 meV must correspond to the V_3 mode, i.e., perpendicular to the axis 1-2-3 of the hourglass in Fig. 12(a) with the V_2 mode parallel to this axis having much lower level spacings on (110), corresponding to ~ 8 meV for ^{2}H.

If one-dimensional square wells and barriers are assumed as in Fig. 14, the wave functions and corresponding matrix elements can be obtained by elementary methods and it can then be attempted to fit the ratio of (D from the ground state of ^{1}H)/(D from the first excited state of ^{2}H)=2.5 together with the requirement that $\epsilon=189$ cal, i.e., ~ 8 meV and that the total repeating unit (well plus barrier) correspond to $a=2.7$ Å. The results for $\theta=0.3$ are a depth of 0.006 eV and a half-width of 0.3 Å for the subsidiary well and a barrier width of 0.25 Å. If the ^{2}H data at $\theta=0.1$ are extrapolated, assuming $\epsilon=8$ meV, the corresponding ratio of diffusion coefficients becomes 0.6. For this case no solutions within the one-dimensional model could be found. It is possible, of course, that for $\theta=0.1$ small ^{1}H contaminations led to a spuriously high value of D for ^{2}H and that the true values lie below the points shown in Fig. 8. However, even if this were so, and if the assignments of dimensions at $\theta=0.3$ are at least qualitatively correct, two difficulties remain. There is no obvious reason, within the model, why tunneling should stop at the first excited state for ^{2}H, or for that matter why tunneling should not also occur from excited states of ^{1}H. If the one-dimensional model (ignoring for the moment the small subsidiary well) is taken at face value, it is straightforward to show that the temperature-dependent overall diffusion coefficient should be given by

$$D(T)=\frac{\frac{1}{a}\sum_i e^{-\epsilon_i/k_BT}D_{\text{tun}}(V-\epsilon_i)+(2\pi mkT/h^2)^{1/2}D_0e^{-V/k_BT}}{\frac{1}{a}\sum_i e^{-\epsilon_i/k_BT}+(2\pi mkT/h^2)^{1/2}e^{-V/k_BT}} \tag{27}$$

if it is recalled that the multiplicity of each state in the well is L/a, L being the (macroscopic) length of the system, and that the one-dimensional partition function is $L(2\pi mkT/h^2)^{1/2}$. The transition from thermal to tunneling diffusion calculated from Eq. (27) is considerably more gradual than that actually found for ^{1}H.

Second, the assignment of well and barrier dimensions amounts to an assignment of matrix elements, and this in turn allows a calculation of D from Eq. (20). The values so calculated exceed the experimental ones by some 6 orders of magnitude. These considerations indicate that the one-dimensional model used so far is too crude and

that the actual two-dimensional nature of the well must be taken into account.

Even a rectangular two-dimensional potential well (as contrasted to a box of infinite depth) is a nontrivial problem since the potential is not separable. It is possible, however, to discuss the situation qualitatively as if a separation into two independent orthogonal degrees of freedom were possible. Then, for the approximate situation shown in Fig. 15 it is clear that along the narrow dimension of the well the energy levels may be quite far apart and that in fact there may be only one bound state for ^{1}H but two or three for ^{2}H. If it is further assumed that tunneling depends much more sensitively on the wave function associated with the narrow dimension, it is clear that tunneling could be very small from the ground state of ^{2}H and would require thermal activation at least to the first excited state, but would occur only from the ground state for ^{1}H. The existence of a small temperature effect for ^{2}H but not for ^{1}H would thus be explained without the explicit assumption of a subsidiary well, although of course the actual potential is much more complicated in shape than either of the approximations we have discussed, so that this point may be moot. The idea that the critical dimension contains only a very small number of bound states can thus explain the otherwise very puzzling sharp transition from thermal to tunneling regimes for ^{1}H as T is decreased and the rather more gradual transition for ^{2}H. As already pointed out, ^{2}H has more bound states than ^{1}H so that thermal-assisted tunneling can occur, leading to a more gradual transition.

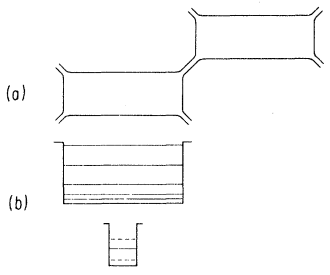

FIG. 15. (a) Schematic top view of proposed two-dimensional well structure. The narrow connecting "neck" between wells is not as deep as the wells but contains the barrier between them. (b) Highly schematic energy-level diagram for a well shown in (a), assuming separability into two degrees of freedom. Solid lines are levels for ^{1}H; dashed lines are levels for ^{2}H. The latter are shown only for the degree of freedom corresponding to the narrow dimension.

Although the above shows how complex the situation is even at low θ, the qualitative conclusion seems correct that the barrier width must be much less than a lattice spacing and probably corresponds to the "necks" between nearest-neighbor W atoms. If this were not so, the ratio of the diffusion coefficient for ^{1}H to that for ^{2}H would have to be very much larger than is the case.

We have already mentioned the discrepancy between the experimental values of D and those calculated with the one-dimensional model. The reason for this discrepancy in the one-dimensional model is clear. In order to reconcile the small difference in D for the two isotopes, quite small barriers must be assumed. Small barriers, on the other hand, lead to large diffusion coefficients. It seems likely that the reason for this apparent paradox is again connected with the essential two-dimensionality of the well. A very simple argument suffices to show this. The tunneling direction, i.e., the direction along which overlap is important is not in fact along either of the well axes but at an angle to them. However, the overlap decreases very rapidly as the coordinate perpendicular to the tunneling direction increases, since both the height and width of the barrier then increase. However, a finite width of the tunneling zone is necessary to obtain finite amplitude, and consequently the competition between decreasing this width and decreasing the penetration probability by increasing it leads to a net decrease in tunneling probability over the one-dimensional case. The argument can easily be made more quantitative, but this does not seem worthwhile in view of the fact that a proper two-dimensional calculation would automatically include this effect.

It seems worth mentioning at this point that preliminary results by Dharmadhikari and Gomer on the (111) plane of W reveal that for certain conditions the transition from thermal to tunneling diffusion for ^{1}H is much more gradual than for the (110) plane. Thus it seems that the effects described here are in fact connected with the details of the potential, as we have assumed.

Phase transitions in the one-component systems

It has already been pointed out that the diffusion coefficients show a pronounced and quite sharp dip at temperatures of 80—90 K, depending on coverage (Fig. 8). We were led to investigate this temperature interval in detail because of sharp

fluctuations in $f_i(0)$, which were seen first. Figures 16—19 show $f_i(0)$ for ^1H and ^2H for various coverages. In each case the fluctuation in $f(0)$ occurs at the temperature of the minimum in D. It seems very plausible to associate the fluctuation in $f(0)$ with a phase transition. In fact, a very simple calculation for a Bragg-Williams lattice gas by Bell, Gomer, and Reiss[8] indicated just such a result. The dip in D can then be interpreted as something akin to critical slowing. Fortuitously, it is possible in the present case to determine the order of the transition. Figure 20 shows that there is a slight change in mean-field-emission current above and below the transition. The reason for this change is not fully understood. However, the dipole layer potential relevant to field emission is that at 0—10 Å from the surface, i.e., very near the actual dipoles. On so local a scale, the potential must depend somewhat on the arrangement of the adsorbate. Thus, it could be slightly different for ordered and disordered arrays, and, in fact, this argues that the phase change observed here corresponds to an order-disorder transition. Incidentally, the variation of $\bar{i}$ with local geometry is very slight, certainly much less than the variation with coverage, so that our method of determining D is still valid, particularly since local rearrangements must occur on time scales much shorter than actual coverage changes by diffusion. Thus, contributions from this effect to the correlation function decay too rapidly to interfere with the diffusional contribution. It is interesting in this connection that in the case of oxygen[6] and CO (Ref. 16), a prediffusive flip-flop with an exponentially decaying correlation function has been observed, while nothing of the kind was seen for H.

In any case the existence of this change in $\bar{i}$ permits quenching and unquenching experiments in

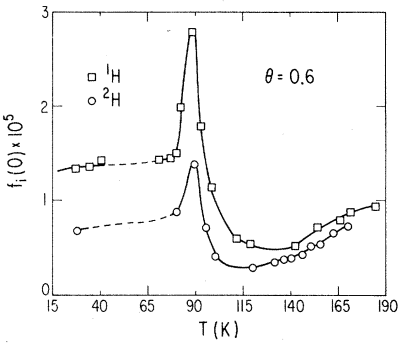

FIG. 17. $f_i(0)$ vs T for hydrogen and deuterium at $\theta=0.6$. To obtain $\langle\delta n^2\rangle/\bar{n}$ multiply $f_i(0)$ by 5.06×10^4.

the case of ^2H, where the changes involved occur slowly enough. Figure 21 shows the change in mean probe-hole current with time for ^2H at $\theta=0.6$ when the emitter was suddenly cooled from 130 to 87 K, or warmed from 80 to 90 K. In both cases $\bar{i}$ changes smoothly at first, then shows a marked plateau, and finally continues to change in the appropriate direction. This halt, indicative of a metastable condition, is typical of first-order transitions.[17] Thus we may conclude that the transition observed is of first order, and most probably corresponds to that from disordered to ordered lattice gas. Figure 22 shows a phase diagram based on these results.

A question of some interest is why the diffusion coefficient is the same above and below the transition. The answer is most probably that the ordered islands are small, or at any rate form and reform constantly so that the effective transport coefficient in the two-phase region is not appreciably different from that in the single phase.

Ordered overlayers with structures $p(2\times1)$, $p(2\times2)$, and $p(1\times1)$ have been reported by LEED

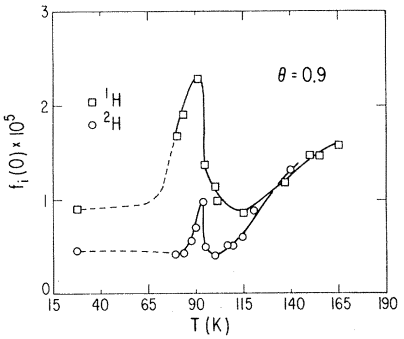

FIG. 16. $f_i(0)$ vs T for hydrogen and deuterium at $\theta=0.9$. To obtain $\langle\delta n^2\rangle/\bar{n}$ multiply $f_i(0)$ by 3.85×10^4.

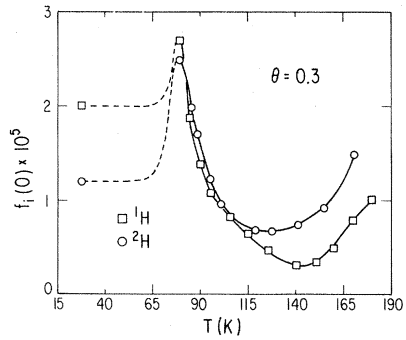

FIG. 18. $f_i(0)$ vs T for hydrogen and deuterium at $\theta=0.3$. To obtain $\langle\delta n^2\rangle/\bar{n}$ multiply $f_i(0)$ by 1.27×10^5.

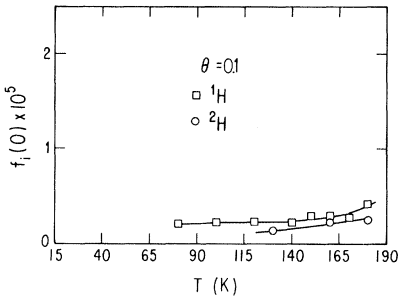

FIG. 19. $f_i(0)$ vs T for hydrogen and deuterium at $\theta=0.1$. To obtain $\langle \delta n^2 \rangle / \bar{n}$ multiply $f_i(0)$ by 4.25×10^5.

for hydrogen on the W(110) plane by Gonchar, Kanash, Naumovets, and Fedorus.[12] These authors also report order-disorder transition temperatures between 200 and 250 K for the $p(2\times1)$ and $p(2\times2)$ layers, respectively. In our work no evidence of such transitions was seen. It is possible, since H is a very weak electron scatterer, that these transitions involve surface reconstruction. It is quite likely that such reconstruction requires a minimum surface size and that reconstructions do not occur on a microscopic (110) plane, i.e., on a field emitter.

Coverage dependence of D_0 in the thermal regime

We turn next to perhaps the most puzzling feature of the present experiments, namely the coverage dependence of D_0 for ^{1}H and ^{2}H. The dependence for ^{1}H is already quite large, spanning 4 orders of magnitude if the data of Fig. 9 can be extrapolated to $\theta=0$. However, this is also the range which was encountered for oxygen on the (110) plane of W,[6] as shown in Fig. 23. For ^{2}H the variation with θ is even more remarkable. For $\theta>0.6$, D_0 continues to increase, reaching values of 5×10^{-2} cm^2 sec^{-1} at $\theta=0.9$, i.e., two additional orders of magnitude above the ^{1}H value. We must

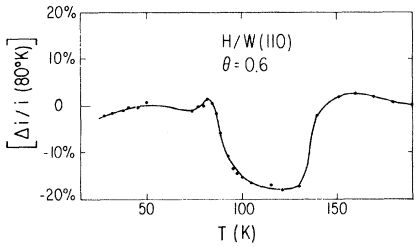

FIG. 20. Mean-field-emission current change Δi divided by mean current $\bar{i}$ at 80 K vs T for $\theta=0.6$.

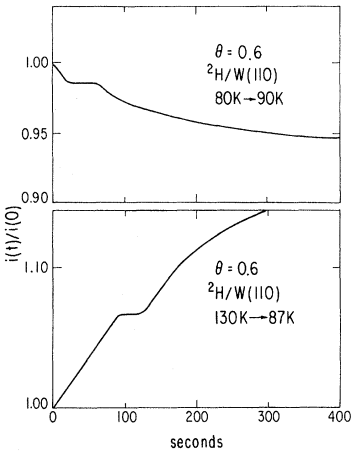

FIG. 21. Supercooling and superheating near the phase transition for deuterium at $\theta=0.6$. The change with time of the mean-field-emission current after the temperature jump is shown.

thus attempt to explain two distinct but related problems. Why does D_0 increase by 4 orders of magnitude with increasing θ for ^{1}H (or O) and why does it increase even more for ^{2}H? We address the second question first. The first thing to note is that the enormous θ dependences for either isotope shrink to less than an order of magnitude in the tunneling regime. Thus they must be connected with the interaction of an activated atom with the nonactivated ones. [Interactions between activated atoms can be wholly neglected, since over the size of the (110) plane there will not be more than one or two such atoms present simultaneously.] Essentially D_0 can be regarded as

$$D_0=\tfrac{1}{4}\lambda^2\nu\,, \tag{28}$$

where λ is an effective mean free path and ν an effective attempt frequency. Although correlation

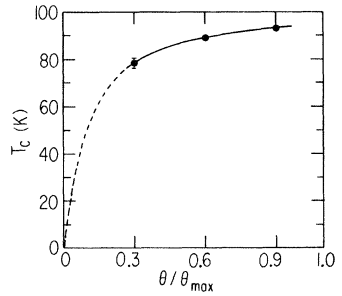

FIG. 22. Proposed phase diagram for the first-order transition. The region above the curve corresponds to disordered, that below to ordered plus disordered lattice gas.

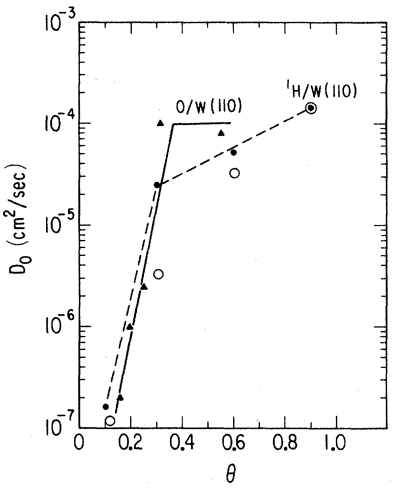

FIG. 23. Plots of $\log_{10}D_0$ vs coverage θ for ^{1}H and O on W(110). The H data are from the present work, those for O from Ref. 6. Also shown is an attempted fit to the H data by Eq. (31), using $b=10$, $c=100$, $d=1000$, $e=1.33\times10^4$ (open circles).

functions measure chemical rather than tracer diffusion coefficients,[9] Eq. (28) is at least qualitatively meaningful even for the chemical diffusion coefficient. It seems unlikely that the differences in mass between ^{1}H and ^{2}H could account for a difference in ν by 2 orders of magnitude at high θ. It seems equally unlikely to assume an effective mean free path much in excess of an atomic jump distance for oxygen at $\theta\leq0.5$. Thus it seems reasonable to assume that the variation from $\sim10^{-8}$ at $\theta=0$ to 10^{-4} cm^{2}sec^{-1} at $\theta=0.5$ for oxygen arises from an increase in effective ν and that the mechanism responsible for this increase is also operative for both H isotopes. (This mechanism will be discussed shortly.) In the case of ^{2}H, however, an additional effect must play a role. We shall now argue that this consists of a substantial increase in λ^2 at $\theta>0.6$. The essence of the argument is the following: For both ^{1}H and ^{2}H the friction coefficient may be expected to be small enough to allow an atom in the activated state to transfer its energy to an H atom in an adjacent well, i.e., to permit forward scattering and thus to lead to an increase in effective mean free path. Classically the process could be described as concerted motion of two adsorbate atoms in adjacent wells, the activated atom entering a filled well and the occupant of that well leaving it in the forward direction. This process could then lead to chains, and clearly the mean chain length will increase as θ increases. However at this point we must take cognizance of the fact that ^{1}H is light enough for quantum statistics to play a role.

It is not obvious *a priori* whether ^{1}H is to be treated as a compound boson and ^{2}H as a compound fermion, or whether only the nuclear statistics matter. If, for instance, the bonding of H to a metal surface can be represented adequately by the immersion of a proton into the electron gas, as in the jellium model, it would seem intuitively correct to worry only about the nuclear statistics. In this case the motion of the proton in any translational or vibrational displacement occurs much more slowly than that of the electrons so that the average electron spin near the proton averages out to zero. For metals like W the jellium description is probably not a very good one, since a bound state seems to separate from the bottom of the conduction band. Nevertheless, we argue that the electron hopping time is very short relative to the nuclear motion and that even for this case only the nuclear spins matter. Thus, we apply Fermi statistics to ^{1}H and Bose statistics to ^{2}H.

For adsorbed ^{1}H the exclusion principle will then prevent substantial overlap of the space parts of the wave functions of two protons in $\frac{3}{4}$ of the cases (spin triplet, spin function symmetric, space function antisymmetric) and allow overlap in only $\frac{1}{4}$ of the cases (spin singlet, spin function antisymmetric, space function symmetric) on average. Thus, if the wave packet of a ^{1}H atom, which has climbed a barrier, overlaps appreciably with the wave function of a ^{1}H atom sitting in the well on the other side of this barrier, the atom on top of the barrier will be prevented from starting its descent into the well, i.e., will not be able to gain the momentum necessary for forward scattering in 75% of all ^{1}H-^{1}H encounters.

For ^{2}H, a boson with spin 1, favorable encounters occur in $\frac{2}{3}$ of the possible cases. Thus the probability of forward scattering for ^{2}H is inherently larger than for ^{1}H. However, this is not enough. If only forward scattering and thus linear chains are assumed, it is shown in the Appendix that the resultant effective mean-square displacement is given by

$$\frac{\langle\lambda^2\rangle}{a^2}=\frac{(1-\theta)}{(1-\beta\theta)}\frac{[2-\alpha(1-\theta)-\theta(1-\beta)]}{[\alpha(1-\theta)+\theta(1-\beta)]^2}\,, \tag{29}$$

where a is a unit lattice displacement (i.e., a single jump length), α the probability that an atom is trapped in an empty site, and β the probability of forward scattering at a full site. For $\alpha=1$, $\beta=1$,

Eq. (29) reduces to

$$\frac{\langle\lambda^2\rangle}{a^2}=\frac{1+\theta}{(1-\theta)^2} \tag{30}$$

which diverges as $\theta\rightarrow 1$. If an atom can be forward scattered right or left with equal probability Eq. (30) is modified only slightly, in that θ in the numerator (*not* denominator) must be replaced by 0.33θ, as shown in the Appendix. For $\theta=0.9$, Eq. (30) leads to an increase in D_0 of 190, i.e., the right order of magnitude required to explain the discrepancy between ^{1}H and ^{2}H. For $\beta=0.25$, i.e., ^{1}H, Eq. (29) predicts negligible effects and even for $\beta=0.66$, i.e., ^{2}H, only a minor increase in D_0 results. Equation (29) also shows that allowing α to be less than unity cannot lead to substantial increases in D_0 *unless* β is close to unity. Thus we must make an additional assumption: We now argue that the mass of ^{2}H is sufficient to make the spatial extent of the deuteron wave packet small enough to allow two adsorbed ^{2}H atoms to approach each other closely enough for forward scattering in nearly all cases, even those where the space parts of the wave functions of the pair are antisymmetric in the exchange. In other words, we argue that ^{1}H because of its light mass must be treated as a quantum particle while ^{2}H is already heavy enough to be treated as a classical particle. One might now ask why chains are not observed with oxygen. The answer is that it is not clear that they are not. Equation (30) shows that chains become important only for $\theta>0.5$. The measurements of Butz and Wagner[18] at high θ do in fact indicate very high values of D_0. These measurements, however, were carried out at much higher temperatures than those of Chen and Gomer[6] for $\theta\leq 0.56$, so that an inherently higher value of the effective jump frequency, with a more positive entropy of activation may have been involved. If chains are absent for adsorbates like oxygen, one would have to invoke large friction coefficients which make the requisite energy transfer improbable.

The hypothesis advanced here for hydrogen suggests that experiments with ^{3}H, a fermion with spin $\frac{1}{2}$, should lead to long chains assuming that the friction coefficient for ^{3}H is still adequately small, because the high mass of ^{3}H would make quantum effects negligible. It is hoped these experiments will be performed in the near future.

We turn now to the increase in D_0 with θ for ^{1}H or O. We have already indicated that the friction coefficients for hydrogen on W may be small, but this is unlikely to be true for oxygen. In any case, we do not believe that this can explain low values of D_0 at low coverage. It is well known that small friction coefficients lead to a reduction in frequency factor for thermal desorption,[19] because this prevents rapid replenishment of particles with high energies from the heat bath once these have been lost by desorption. However in diffusion particles are not lost, since they are able to enter adjacent wells. Consequently, for the zero friction case, an equilibrium population in the activated state is established, and the diffusion coefficient is given by Eq. (17) (modified to take account of this population) with v_g a thermal velocity and λ given by Eq. (18). Thus D_0 would be expected to *increase* as θ decreases.[20] A possible explanation is the following: It is known that adsorption at low coverage can lead to some distortion in the position of substrate atoms in the immediate vicinity of the adsorbate. At high coverage these distortions disappear because the presence of other adsorbate atoms restores the original symmetry of forces acting on the substrate atoms. It is then possible that at low coverage diffusion involves the carrying along of this distortion, or "polarons." The requisite concerted motion of substrate and adsorbate atoms then results in a decrease in D_0 over that which would result if the substrate concerted motion were absent. As θ increases, the forces exerted by other adsorbate atoms inhibit the polaron contribution to diffusion and D_0 increases. The increase in D_0 may, but need not necessarily be, accompanied by an increase in activation energy. To the extent that the absence of polaron effects increases E, one would expect an increase. However, it is also possible that part of the substrate motion tending to reduce D_0, which is inhibited by other adsorbate atoms, is not directly connected with an increase in E (or possibly with so high an increase as to give no weight to diffusion channels which avoid it at low θ). In the present case the change in D_0 for ^{1}H from low to high θ is $\sim 10^4$. If this were to be accounted for purely in terms of an increase in E, this would have to be 2 kcal, taking a mean temperature of 160 K. The actual increase from $\theta=0.1$ to 0.9 observed is 1 kcal, i.e., 50% of what would be required. In the case of oxygen on W, essentially all the change in D_0 can be attributed to a factor $e^{-\Delta E/k_BT}$.

This "polaron" effect is not necessarily a static one. Other adatoms could couple to the motion of the diffusing adatom and its substrate neighbors in such a way as to make the latter seem rigid to the

diffusing atom. Such dynamical correlations must in fact be invoked to explain the D_0 behavior of hydrogen-deuterium mixtures, described in a subsequent section: For total $\theta=0.9$ equimolar mixtures, or mixtures richer in hydrogen than deuterium, show D_0 values which correspond more to those of the individual, not total coverage. This can be reconciled with the present model by assuming that deuterium is not effective in increasing D_0 for hydrogen and vice versa, because of the differences in the relevant vibrational frequencies.

The argument can be made more quantitative. Suppose that we assume two nearest- and two (pseudo) next-nearest-neighbor atoms (to the jumping adatom) to contribute. We can then assign various weights to the D_0 (i.e., effective ν) values depending on which configurations occur. The result would be

$$D_0(\theta)/D_0(0)=(1-\theta)^4+b\,2\theta(1-\theta)^3+c\theta^2(1-\theta)^2+d\,4\theta^3(1-\theta)+e\theta^4\,, \tag{31}$$

where c is a composite of the various possibilities with two empty and two full sites of the four relevant ones. The best fit of Eq. (31) to the ^{1}H prefactor is shown in Fig. 23 with the restriction that none of the coefficients b,c,d,e can be negative (which would be unphysical). The fit is not very good, for a simple physical reason: The weights given by Eq. (31) to various configurations are correct only at $T=\infty$ or if there are no adsorbate-adsorbate interactions. The latter will lead to various clusterings whose net effect will be to increase the probability of certain configurations even at low θ values, thus increasing $D_0(\theta)$ above the values predicted by Eq. (31). The effect is even more pronounced for oxygen, where a leveling off in D_0 occurs at roughly the coverage where the $p(2\times1)$ structure is known to predominate.

Thus the present model provides at least a qualitative explanation for the increase in D_0 for classical ad particles. In the case of ^{2}H it is necessary to invoke this mechanism also, of course, to get from $D_0=10^{-8}$ to 10^{-4} cm^2 sec^{-1}. Once the chain-initiating jump (whose probability increases with θ as just postulated) has occurred, the chain then propagates so that the effects are multiplicative or additive on a semilog plot. Since chains become important only at high θ, where D_0 is already high relative to the $\theta=0$ value, the chain propagating steps can be expected to have high probabilities also, or more precisely not to be inhibited by polaron effects at high coverages.

Mean-square fluctuations

If the absolute adsorbate density is known, it is possible to obtain $f_n(0)=\delta n^2$ from $f_i(0)$ and Eq. (3). As indicated by Eq. (8), $f_n(0)$ is related to the compressibility of the ad phase and thus of some interest. It seems very probable from the LEED results of Ref. 12, which lead to a $p(1\times1)$ pattern at saturation, that $\theta=1$ corresponds to H/W=1, i.e., to $c_H=1.4\times10^{15}$ atoms/cm^2. On this basis the $f_i(0)$ values shown in Figs. 16–19 can be converted by the indicated factors to $f_n(0)/\bar{n}$ where $\bar{n}$ is the average number of H atoms in the probed region computed from c and the area A of this region. As shown, for instance, by Eq. (21) of Ref. 8,

$$\langle\delta n^2\rangle/\bar{n}=\frac{1-\theta}{1+2\eta\theta(1-\theta)} \tag{32}$$

for a lattice gas without correlations. Here $\theta=$H/W, i.e., fractional coverage, and $\eta=\epsilon_i/k_BT$ where ϵ_i is the nearest-neighbor-interaction energy. Thus for $\epsilon_i=0$

$$\langle\delta n^2\rangle/\bar{n}=1-\theta\,. \tag{33}$$

The data of Figs. 16–19 are summarized in Tables II and III and show some interesting trends. First, below the first-order transition temperature $f_n(0)/[\bar{n}(1-\theta)]$ is temperature independent and seems to approach unity as $\theta\to0$. $f_n(0)/[\bar{n}(1-\theta)]$ seems to have a maximum at $\theta=0.3$ for both ^{1}H and ^{2}H. It is interesting that the values for ^{2}H seem to be significantly smaller than for ^{1}H at all θ. This must be connected either with the smaller zero-point energy for ^{2}H or with the statistics. Figures 16–18 also show that the maximum in the $f(0)$ curves near the first-order phase transition is consistently higher for ^{1}H than for ^{2}H. Above the transition $f(0)$ increases with T, and this increase is exponential, as indicated by Fig. 24. This situation is similar to that encountered for oxygen on the (110) plane.[6] For oxygen the increase in $f(0)$ was followed at even higher temperatures by a decrease. In the present case this was seen only for ^{2}H at $\theta=0.3$, but it is likely that a similar trend would have been seen at other coverages if T could have been increased sufficiently without loss of adsorbate. The exponential regimes lead to energies E, crudely associable with repulsive ad-ad interactions listed in Table II. If $f_n(0)$ is assumed to have the form

TABLE II. Mean-square fluctuations at 140 K.

Isotope	θ	$\langle \delta n^2 \rangle / [\bar{n}(1-\theta)]$	E (kcal)	$\langle \delta n^2 \rangle e^{E/k_B T} / [\bar{n}(1-\theta)]$
^{1}H	0.1	0.94		0.94
	0.3	0.57	2.0	720
	0.6	0.66	0.74	9.2
	0.9	5.1	0.48	29
^{2}H	0.1	0.9		0.9
	0.3	1.31	1.0	46
	0.6	0.65	0.91	17
	0.9	3.3	1.0	109

$$\langle \delta n^2 \rangle = \bar{n}(1-\theta) e^{-E/k_B T}, \tag{34}$$

then $e^{E/k_B T} \langle \delta n^2 \rangle / [\bar{n}(1-\theta)]$ should be unity. Table II shows that this is far from being the case. Consequently $f_n(0)$ must have a much more complicated form than Eq. (34) in the disordered regime.

Hydrogen-deuterium mixtures

Some experiments were also carried out on mixtures of ^{1}H and ^{2}H. In order to establish known coverages of each isotope in the mixture, two procedures were used which gave identical results. First, equal pressures of hydrogen and deuterium, as measured on the ion gauge, were admitted to the system (2.5×10^{-9} torr of each), the emitter flashed clean, immediately cooled to 300 K, and dosing allowed to proceed until the desired total coverage $\theta = 0.9$ was reached, as determined from emission measurements. The emitter was then cooled and the gas pumped out. In a check on this method, the above procedure was carried out in identical fashion but with hydrogen or with deuterium

TABLE III. Mean-square fluctuation below phase transition.

Isotope	θ	$\dfrac{\langle \delta n^2 \rangle}{\bar{n}(1-\theta)}$
^{1}H	0.1	0.94
	0.3	3.4
	0.6	1.6
	0.9	3.5
^{2}H	0.1	0.71
	0.3	2.2
	0.6	1.0
	0.9	1.9

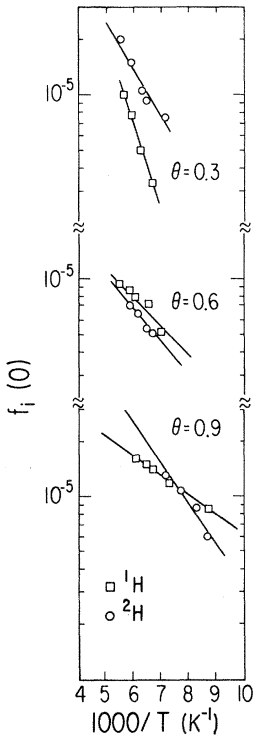

FIG. 24. Plots of $\log_{10} f_i(0)$ vs $1/T$ for hydrogen and deuterium in the thermally activated diffusion regime.

alone, each at a pressure of 5×10^{-9} torr. In this way the total work-function increment obtained with the mixture was found for each gas, suggesting either (a) no interference between ^1H and ^2H diffusion, plus comparable sticking coefficients on the rough planes of the emitter, *or* (b) a compensation between increased sticking coefficient and decreased diffusion coefficients for ^2H. In the second method, the emitter was first dosed with ^1H, which was then totally equilibrated over the entire emitter. The emitter was then dosed with deuterium and the latter allowed to diffuse into the (110) plane as in procedure 1. Again the same final work-function increment was obtained. Thus it appears established that known relative partial coverages of ^1H and ^2H can be obtained by dosing with known partial pressures. Experiments at total $\theta=0.9$ were carried out with three compositions: 75 at.% ^2H, 25 at.% ^1H; 50 at.% ^1H, 50 at.% ^2H; 25 at.% ^2H, 75 at.% ^1H.

The results are shown in Fig. 25 for the diffusion coefficients and in Fig. 26 for $f_i(0)$. For 75 at.% ^1H, 25 at.% ^2H, and 50 at.% ^1H, 50 at.% ^2H mixtures at total $\theta=0.9$ the results in the activated regime lie fairly close to the curves for $\theta=0.6$ of the pure components, but actually yield values of $D_0=3.5\times10^{-6}$ and 2.7×10^{-6} cm^2/sec, respectively, and $E=4.0$ kcal/mole in each case. These values are lower than for ^1H at $\theta=0.45$ and 0.67, respectively. For $\theta=0.9$, 25 at.% ^1H, 75 at.% ^2H somewhat different behavior occurs in that $E=7.4$ kcal and $D_0=0.4$ cm^2/sec. Despite the high apparent E the overall value of D is higher than for the other mixtures.

As T decreases there is observed in all cases a dip in D. Associated with this dip is also a fluctuation in $f(0)$ as indicated by Fig. 26. For $\theta=0.9$, 50 at.% ^1H, 50 at.% ^2H, the transition through this dip occurred so rapidly that it could be followed on an oscilloscope displaying the fluctuations as T was varied. Attempts to look for a change in mean current above and below the dip were negative. It is also interesting to note that the temperature of lowest D corresponds to the inflection point of the $f(0)$ fluctuation. As T was lowered even further, the first-order transition already seen with pure phases also occurred. It seems plausible to interpret the dip in D and the concomitant irregularity in $f(0)$ as a phase segregation between ^1H and ^2H at $T\cong130$ K. This does not correspond, however, to ordering within each component region; this occurs only at the "normal" transition temperature 80–90 K.

As already pointed out, after segregation the total D can be explained by assuming that each component behaves roughly as if it occupied its own region of the surface and thus had a D corresponding to, in the case of 50%-50% mixtures for instance, $\theta=0.9$ and so on, with the observed correlation function a mean of the D values of each isotope.

Some experiments were also carried out for 50%-50% mixtures at total $\theta=0.3$. Here qualitatively similar results, including a dip in D at

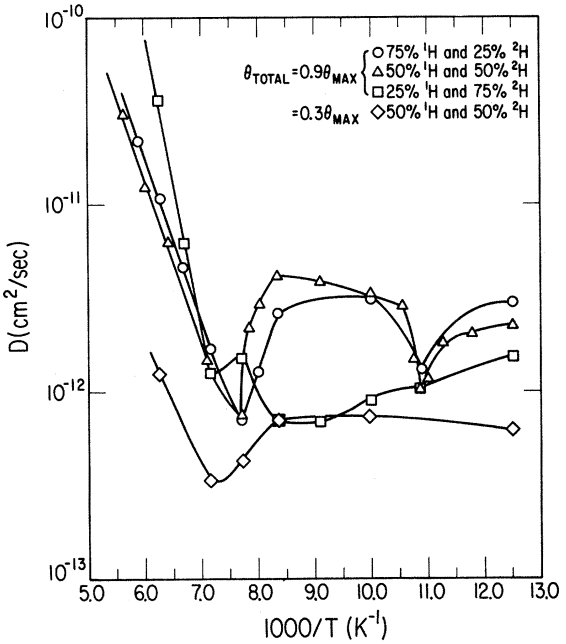

FIG. 25. Plots of $\log_{10}D$ vs $1/T$ for various hydrogen-deuterium mixtures, as indicated on the figure. The concentration is expressed in atomic percent.

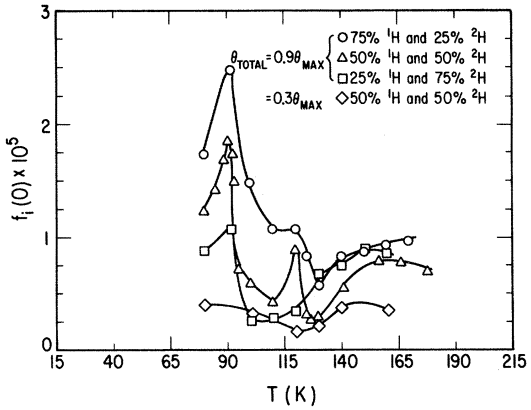

FIG. 26. $f_i(0)$ vs T for various hydrogen-deuterium mixtures, as indicated on the figure. Concentrations are expressed in atomic percent.

$T=139$ K, i.e., *higher* than those for $\theta=0.9$ were found. The low-temperature value of D, however, is 7×10^{-13} cm^2/sec, which is an order of magnitude smaller than D for ^{1}H at $\theta=0.3$. In this case, therefore, a rather different phenomenon may have occurred, namely a nonsegregated freezing in of ^{2}H and thus an impeding of ^{1}H diffusion rather than a true segregation. Phase segregations must be driven thermodynamically by the fact that the two isotopes have different compressibilites, as indicated by the difference in $f(0)$, and it seems reasonable that it is not as strongly driven and may not occur at all at low total coverages.

In view of the chain mechanism proposed for the high values of D_0 found for ^{2}H at high θ, we must ask why mixtures at high total θ show no evidence of this behavior except for very high ^{2}H content. The question becomes relevant since there is no statistical prohibition of any kind on ^{1}H-^{2}H interactions. The answer is probably that energy and momentum conservation requires that $\frac{8}{9}$ of the energy of the scattering atom be transferred to the scattered one in both ^{1}H-^{2}H and ^{2}H-^{1}H collisions. Thus atoms with just sufficient energy to overcome the barrier cannot propagate chains if these would have to involve hydrogen-deuterium collisions, which would be the case when the hydrogen content is appreciable. Since the activation energy for deuterium could conceivably scatter hydrogen, but not vice versa. For this case ^{1}H-^{1}H collisions would still act as chain stoppers and result in very short effective chain lengths. It is possible to work out an expression for $\langle\lambda^2\rangle/a^2$ for this case, as indicated in the Appendix:

$$\frac{\langle\lambda^2\rangle}{a^2}=\frac{\theta_D}{\theta_t}\frac{(1-\theta_t)(1+\theta_D)}{(1-\theta_D)^3}+\frac{\theta_D}{\theta_t}\frac{(1-\theta_t)\theta_H}{(1-\theta_D)(1-\beta\theta_H)}\left[\frac{1+\theta_D}{(1-\theta_D)^2}+\frac{1+\beta\theta_H}{(1-\beta\theta_H)^2}+\frac{2}{(1-\theta_D)(1-\beta\theta_H)}\right]+\frac{\theta_H}{\theta_t}\frac{(1-\theta_t)}{\beta}\left[\beta-1+\frac{1+\beta\theta_H}{(1-\beta\theta_H)^3}\right], \tag{35}$$

where β stands for $\beta_H=0.25$ and θ_H and θ_D stand for the coverages of ^{1}H and ^{2}H, respectively.

The result confirms that for 50%-50% mixtures at total $\theta=0.9$ only a negligible increase in D_0 occurs. However, for $\theta_{tot}=0.9$, 75 at.% ^{2}H−25 at.% ^{1}H an activation energy of 7.4 kcal and a high D_0 value are observed and this requires discussion. The following explanation seems, at least qualitatively, plausible. If the energy transfer restriction was not important, long chains could result if ^{1}H-^{1}H chain-stopping collisions were not too frequent, i.e., if the ^{1}H concentration were sufficiently low. In order to achieve this, however, all that is needed is more energy.

Thus the overall D may be maximized by a higher activation energy and a resultant gain in chain length, i.e., λ^2. It is shown in the Appendix that $\langle\lambda_2^2\rangle$ can be approximated by

$$\frac{\langle\lambda_2^2\rangle}{a^2}\simeq\frac{\theta_D(1-\theta_t)(1+\theta_D+\theta_D\theta_H)}{\theta_t[1-\theta_D(1+\theta_H)]^3}+\frac{\theta_H(1-\theta_t)(1+\theta_D)}{\theta_t(1-\theta_D)^3} \tag{36}$$

for "hot" atom chain initiation. The observed value of D would then be given by

$$D=\langle\lambda_1^2\rangle\nu_1 e^{-E_1/k_BT}+\langle\lambda_2^2\rangle\nu_2 e^{-E_2/k_BT}, \tag{37}$$

where the subscripts 1 and 2 refer to "cold" and "hot" atom initiated processes. $\langle\lambda_2^2\rangle$ for $\theta_D=0.675$, $\theta_H=0.225$ turns out to be $28a^2$ and for $\theta_D=\theta_H=0.45$ to be $2a^2$. If ν_2 were no larger than ν_1 it is clear that a gain of ~30 would not be enough to offset the Boltzmann factor $e^{-2500/2T}=4\times10^{-4}$, which is the price of achieving the longer chains. However, the extra activation energy also buys a positive entropy of activation; in fact the hot atom can be considered to have effectively 2 degrees of translational freedom. It is not hard to see that this will increase ν_2 to the point of making the overall value of D larger by inclusion of "hot" atom initiated chains than it would be without this contribution. It is also reasonable that for higher ^{1}H coverages, for instance $\theta_H=\theta_D=0.45$, the small chain length resulting from hot atoms is not enough, even with the increase in ν_2, to make hot atom contributions significant.

CONCLUSION

This paper has presented a number of diffusion results for hydrogen and deuterium on the (110)

plane of tungsten. Almost none of the results found were anticipated, and most do not have, at this time, a wholly satisfactory explanation. Nevertheless the results suggest several interesting things. First, there are isotope, and probably statistics-dependent interactions in thermally activated diffusion at temperatures of $T > 130$ K where one would not, offhand, have expected statistics to play a role. Probably this comes about because of the high local density during the actual interaction, i.e., scattering event. Second, there is adsorbate tunneling, and even here there are significant differences between the two isotopes which cannot be explained on the basis of mass alone; i.e., adsorbate-adsorbate interactions play a role in this regime also. Third, there is clear evidence for a first-order phase transition in the pure one-component systems. Finally, mixtures give evidence of a segregation, which seems complete for high total coverages and apparently incomplete for low total coverage. It is fairly clear that considerable theoretical effort will be required to explain these results in more detail. It is hoped that this paper will stimulate interest in such efforts.

ACKNOWLEDGMENTS

It is a pleasure to thank a number of colleagues for stimulating discussions, principally M. H. Cohen and L. Nosanow. The computer calculations on various well and barrier models were carried out by Dr. J. R. Banavar, and more extensively by Dr. D. Bowman, whose help is hereby gratefully acknowledged. This work was supported in part by NSF Grant No. CHE8007999 and its predecessor NSF Grant No. CHE77-08328. We have also benefited from the Materials Research Laboratory of the National Science Foundation at the University of Chicago.

APPENDIX

We sketch here the derivation of the expressions for mean-square chain length under various conditions.

(1) Single species. We assume that there is a probability α that an activated atom will stop at an empty site, $1-\alpha$ that it will go past this site, and that the probability of forward scattering when an activated atom or one which has been kicked out of its site encounters a full site is β. We further assume that a chain can only propagate if all necessary collisions are favorable. We shall also consider all chains in units of the elementary jump length a.

The probability of zero chain length is then

$$P_0=(1-\beta)(\theta+\beta\theta^2+\beta^2\theta^3+\cdots)=\frac{(1-\beta)\theta}{1-\beta\theta} . \tag{A1}$$

The probability of a chain of length $n=1$ is

$$P_1=\alpha(1-\theta)+(1-\alpha)(1-\theta)P_0 \tag{A2}$$

and

$$P_m=[\beta\theta+(1-\alpha)(1-\theta)]P_{m-1} . \tag{A3}$$

Thus

$$\sum_0^\infty P_n=P_0+P_1\sum_0^\infty[\beta\theta+(1-\alpha)(1-\theta)]^n \tag{A4}$$

which can readily be shown to equal unity. $\langle\lambda^2\rangle/a^2$ is then given by

$$\frac{\langle\lambda^2\rangle}{a^2}=\sum_0^\infty n^2P_n , \tag{A5}$$

since the $n=0$ term does not contribute. Thus

$$\frac{\langle\lambda^2\rangle}{a^2}=P_1\sum_0^\infty n^2[\beta\theta+(1-\alpha)(1-\theta)]^{n-1} . \tag{A6}$$

The sum is evaluated by using the identity

$$\sum_0^\infty n^2x^n\equiv x^2\frac{\partial^2}{\partial x^2}\sum_0^\infty x^n+x\frac{\partial}{\partial x}\sum_0^\infty x^n \tag{A7}$$

and leads to Eq. (29).

(2) Cold mixtures. Here we assume for simplicity that $\alpha=1$ and that $\beta_D=1$. (The letters H and D in this and the next section refer to ^{1}H and ^{2}H, respectively.) We shall label $\beta_H=\beta$ for simplicity of notation. We assume that forward scattering of H or D by D is always allowed, but that scattering of D by H is never allowed. Further, the usual restriction $\beta=0.25$ applies to scattering of H by H. We then obtain the recursion relations for $n\geq 2$:

$$P_n^D=\theta_HP_{n-1}^H+\theta_DP_{n-1}^D , \tag{A8}$$

$$P_n^H=\beta^{n-2}\theta_H^{n-1}(1-\theta_t) . \tag{A9}$$

Here P_n^D means a chain initiated by a D atom of total length n, and P_n^H a chain of length n initiated by an H atom. P_1 is given simply by

$$P_1^H=P_1^D=1-\theta_{tot} \tag{A10}$$

where θ_{tot} stands for total coverage, i.e., $\theta_{tot}=\theta_H+\theta_D$. We then find for the mean chain length resulting from D-initiated chains

$$\frac{\langle\lambda_D^2\rangle}{a^2}=(1-\theta_{tot})\sum_1^\infty n^2\theta_D^{n-1}+(1-\theta_{tot})\sum_{\substack{n=2\\1\le m\le n-1}}^\infty n^2\theta_D^{n-m-1}\beta^{m-1}\theta_H^m$$

$$=(1-\theta_{tot})\sum_1^\infty n^2\theta_D^{n-1}+\frac{1-\theta_{tot}}{\beta\theta_D}\sum_{\substack{n=2\\1\le m\le n-1}}^\infty n^2\theta_D^{n-m}(\beta\theta_H)^m\ . \tag{A11}$$

The first term is easily evaluated. The summation in the second term can be shown by an extension of Eq. (A7) to have the form

$$\sum n^2x^{n-m}y^m=(\,x^2D_{xx}+xD_x+2xyD_{xy}+yD_y+y^2D_{yy})\sum x^{n-m}y^m\ , \tag{A12}$$

where $x=\theta_D$, $y=\beta\theta_H$, and $D_{xx}\equiv\frac{\partial^2}{\partial x^2}$, etc. The sum

$$\sum_{\substack{n=2\\1<m<n-1}}^\infty x^{n-m}y^m=\sum_{n=2}^\infty x^n\sum_{m=1}^{n-1}(y/x)^m=\frac{xy}{(1-x)(1-y)} \tag{A13}$$

by straightforward algebra. $\langle\lambda_D^2\rangle/a^2$ is then readily obtained as is $\langle\lambda_H^2\rangle/a^2$. The final result is

$$\frac{\langle\lambda^2\rangle}{a^2}=\frac{\theta_D}{\theta_{tot}}\frac{\langle\lambda_D^2\rangle}{a^2}+\frac{\theta_H}{\theta_{tot}}\frac{\langle\lambda_H^2\rangle}{a^2} \tag{A14}$$

which is given explicitly by Eq. (35) of the text. It should be noted that the contribution from $\langle\lambda_H^2\rangle$ is negligible as expected. The net result is of the same order of magnitude as if only D atoms at θ_D were present. This justifies the assumption $\alpha=1$ in this case, since letting $\alpha<1$ would not substantially increase $\langle\lambda^2\rangle$ at this low value of θ (unless $\alpha<<1$, which is unlikely).

(3) "Hot" atom initiated chains. We assume that there are no restrictions on H-D or D-H scattering, and allow chains like H-D-H-D-.... That is, we assume that if a D atom was forward scattered by an H atom it has enough energy to scatter an H atom and to impart sufficient energy to the latter to allow that H atom to scatter another D atom in turn. We place the usual restrictions of $\beta=0.25$ on H-H collisions. We then find

$$P_n^H=\beta\theta_HP_{n-1}^H+\theta_DP_{n-1}^D\ , \tag{A15}$$

$$P_n^D=\theta_DP_{n-1}^D+\theta_HP_{n-1}^H\ . \tag{A16}$$

If we now neglect the relatively unimportant piece $\beta\theta_HP_{n-1}^H$ in P_n^H we have approximately

$$P_n^D\cong\theta_D(1+\theta_H)P_{n-1}^D\ , \tag{A17}$$

$$P_n^H\cong\theta_DP_{n-1}^D\ , \tag{A18}$$

so that

$$\frac{\langle\lambda^2\rangle}{a^2}=\frac{\theta_D}{\theta_{tot}}\sum_{n=1}^\infty n^2[\theta_D(1+\theta_H)]^{n-1}P_1^D+\frac{\theta_H}{\theta_{tot}}\sum_{n=1}^\infty n^2\theta_D^{n-1}P_1^D\ , \tag{A19}$$

with

$$P_1^D=1-\theta_{tot} \tag{A20}$$

so that Eq. (36) is easily obtained.

(4) Branching chains. All the models considered so far treat forward scattering in only one direction. Examination of Fig. 12 indicates, however, that it may be almost as probable for the scattered atom to go "left" as to go "right," still in a forward direction. For the analog of Eq. (30) of the main text, i.e., $\alpha=\beta=1$, it is easy to show that the correction to $\langle\lambda^2\rangle$ from this possibility is not large.

The probability of a particular chain of n jumps, q to the right, p to the left, is

$$P_n=(\theta/2)^{n-1}\tfrac{1}{2}(1-\theta) \tag{A21}$$

if the probabilities of going to right or left are equal. The total number of ways in which n jumps can be made with a right-left choice at each branch point is 2^n. The mean-square displacement from the origin for chains of n jumps is $\langle\lambda^2\rangle_n$

$$\langle\lambda^2\rangle_n=\langle p^2\rangle+\langle q^2\rangle-2\langle pq\rangle\cos\epsilon\ , \tag{A22}$$

where $\epsilon=109.47°$ is the angle between lattice rows, so that $\cos\epsilon=-0.33$.

Since p and q can be considered to be the number of steps to left and right in a random walk of n jumps we have

$$\langle\,|p-q|^2\rangle=n \tag{A23}$$

and we also have that

$$p+q=n\ . \tag{A24}$$

Expanding Eq. (A23), squaring Eq. (A24), and then taking averages yields

$$2\langle pq\rangle=(n^2-n)/2 \tag{A25}$$

so that, using (A24) and (A25),

$$\langle\lambda\rangle_n^2=\tfrac{1}{2}n^2(1-\cos\epsilon)+\tfrac{1}{2}n(1+\cos\epsilon)\ . \tag{A26}$$

Thus

$$\langle\lambda^2\rangle/a^2=\tfrac{1}{2}(1-\theta)\sum_0^\infty[\,n^2\theta^{n-1}(1-\cos\epsilon)+n\theta^{n-1}(1+\cos\epsilon)]\ , \tag{A27}$$

which is easily evaluated to give

$$\langle\lambda^2\rangle/a^2=(1+0.33\theta)/(1-\theta)^2\ . \tag{A28}$$

---

*Present address: Bellaire Research Center, Shell Oil Company, P.O. Box 481, Houston, Texas 77001.

[1]R. Wortman, R. Gomer, and R. Lundy, J. Chem. Phys. 27, 1099 (1957).
[2]R. Gomer, R. Wortman, and R. Lundy, J. Chem. Phys. 26, 1147 (1957).
[3]R. Gomer, Surf, Sci. 38, 373 (1973).
[4]R. DiFoggio and R. Gomer, Phys. Rev. Lett. 44, 1258 (1980).
[5]R. DiFoggio and R. Gomer, in *Ordering in Two Dimensions,* edited by S. K. Sinha (North-Holland, New York, 1980), p. 235.
[6]J. -R. Chen and R. Gomer, Surf. Sci. 79, 413 (1979).
[7]R. Gomer, *Field Emission and Field Ionization* (Harvard Universtiy Press, Cambridge, Mass., 1961).
[8]B. Bell, R. Gomer, and H. Reiss, Surf. Sci. 55, 494 (1976).
[9]G. Mazenko, J. R. Banavar, and R. Gomer, Surf. Sci. 107, 459 (1981).
[10]R. S. Polizzotti and G. Ehrlich, J. Chem. Phys. 71, 259 (1979).
[11]E. W. Plummer and A. E. Bell, J. Vac. Sci. Technol. 9, 583 (1972).
[12]V. V. Gonchar, O. V. Kanash, A. G. Naumovets, and A. G. Fedorus, Zh. Eksp. Teor. Fiz. Pis'ma Red. 28, 358 (1978) [JETP Lett. 28, 330 (1978)].
[13]D. Menzel (private communication).
[14]C. Backx, B. Feuerbacher, B. Fitton, and R. F. Willis, Phys. Lett. 60A, 145 (1977).
[15]W. Ho, R. F. Willis, and E. W. Plummer, Phys. Rev. Lett. 40, 1463 (1978).
[16]J. -R. Chen and R. Gomer, Surf. Sci. 81, 589 (1979).
[17]D. P. Landau and K. Binder, Phys. Rev. B 17, 2328 (1978).
[18]R. Butz and H. Wagner, Surf. Sci. 63, 448 (1977).
[19]See, for instance, G. Iche and Ph. Nozières, J. Phys. (Paris) 37, 1313 (1976).
[20]J. R. Banavar, M. H. Cohen, and R. Gomer, Surf. Sci. 107, 113 (1981).